IET Generation, Transmission & Distribution

Research Article

ISSN 1751-8687
Received on 23rd November 2017
Revised 31st January 2018
Accepted on 17th February 2018
E-First on 22nd March 2018
doi: 10.1049/iet-gtd.2017.1829
www.ietdl.org

Impacts of the model uncertainty on the voltage regulation problem of medium-voltage distribution systems

Bashir Bakhshideh Zad[1] ✉, Jacques Lobry[1], François Vallée[1]
[1]Department of Electrical Engineering, University of Mons, No. 31, Boulevard Dolez, Mons, Belgium
✉ *E-mail: Bashir.BAKHSHIDEHZAD@umons.ac.be*

Abstract: In this paper, a novel framework is proposed in order to evaluate impacts of the uncertain models of the system components on the voltage regulation problem of the medium-voltage distribution systems. The investigation focuses on the model uncertainty associated with voltage dependency of loads, power factor of loads, thermal dependency of lines, shunt admittances of lines and internal resistance of substation transformer. To this end, firstly, voltage constraints are managed using a centralised voltage control algorithm (VCA) by relying on the simplified models of the system components. The system loads and lines as well as the substation transformer are then modelled with the uncertain variables which are bounded in the predefined ranges. Monte Carlo (MC) simulations are used to create wide series of scenarios that cover the possible values that the parameters of the system components can take due to their uncertain nature. The model uncertainty impacts on the voltage regulation problem are finally evaluated by the load flow calculations considering the scenarios created by the MC simulations and the set-point obtained by the VCA. The proposed investigation brings useful information regarding the possible deviations that the node voltages can have due to the uncertain models of the studied components.

1 Introduction

The massive integration of distributed generation units (DGUs) into the electric distribution systems has created serious technical problems for the distribution system operators. To deal with such arising issues, the conventional passive manner of the distribution network management is being replaced by the active network management schemes aiming at operating network in a safe and cost-effective way by taking advantage of the real-time communication and optimal control of the available devices. In this context, a more comprehensive and detailed analysis of the distribution system is needed to be carried out.

Voltage regulation problem is one of the main challenges in the distribution systems integrating a high level of DGUs. Different voltage control schemes have been proposed in the literature in order to remove the voltage violations and to keep the system voltages within the predefined limits. The proposed voltage control algorithms (VCAs) can be classified into the centralised or distributed algorithm that employs the transformer tap changer [1–4], active and reactive powers control of DGUs [1–9], energy storage [10] and circuit breakers [1].

Despite the differences of the existing VCAs, they have been developed relying on similar assumptions that the loads are voltage independent [1, 3–11], exact load power factors (PFs) are available [1–11], system lines are equivalent to the series impedances [2, 5, 6, 9, 10] which have constant values over the time [1–10] and the substation transformer is a pure reactance [2, 5, 9] that can be even negligible [4, 6]. In reality, however, these assumptions do not hold since the load powers are in function of the voltage, load PFs may be different from the ones considered in the load models, shunt admittances of the lines cannot be neglected, branch resistances vary with respect to the conductor temperatures and internal resistance of the substation transformer is needed to be taken into account. Therefore, the models based on which the VCAs in [1–10] were developed do not represent the real characteristics of the network components. Consequently, corrective decisions of the VCA obtained by relying on the simplified network model may be insufficient to solve a specific voltage violation problem of the real case. A VCA based on the robust optimisation has been developed in [11] to deal with the uncertain model of the line resistances due to the thermal dependency effect.

In this paper, a framework is proposed in order to evaluate impacts of the uncertainties associated with the voltage dependency of loads, PF of loads, the thermal dependency of lines, shunt admittances of lines and internal resistance of the substation transformer on the output results of the studied VCA. The voltage regulation problem is first solved by relying on the simplified models of the system components. Due to the fact that the exact and up-to-date models of the network components are not available, the studied components are considered with the uncertain variables which are bounded in the predefined ranges. The Monte Carlo (MC) simulations are used to create wide series of scenarios that characterise the uncertain models of the studied components. The uncertainty impacts associated with the models of the studied components on the voltage constraints of the VCA are evaluated by the load flow calculations. The Newton–Raphson load flow (NRLF) study is reformulated in this regard in order to incorporate the effect of the voltage dependency of the loads. Evaluating the cumulative uncertainty effects of the studied components brings us useful information regarding the maximum deviations that the node voltages can have from the values obtained by the VCA. This can be utilised in order to reset the targeted bounds of the VCA such that it makes the VCA solutions robust against the uncertainty of the system components model.

The rest of this paper is organised as follows. In Section 2, the proposed method is described by focusing on the studied VCA, the scenarios' creation technique using MC simulations and the NRLF study. In Section 3, the studied cases are presented that is followed by introducing the investigated test system in Section 4. Then, the simulation results are presented and discussed in Section 5. In the end, the conclusion is reported in Section 6.

2 Proposed method in order to evaluate impacts of the model uncertainty on the voltage constraints

In this work, the VCA presented in [9, 12] is used to provide the basic set of the voltage results. The VCA is designed to return the system voltages within the permitted voltage range in case of having voltage violations. A priori, it is expected that in the output point of the VCA, the voltage constraints are managed and the system voltages are returned to the permitted voltage range. However, in the VCA, system loads are assumed to be voltage

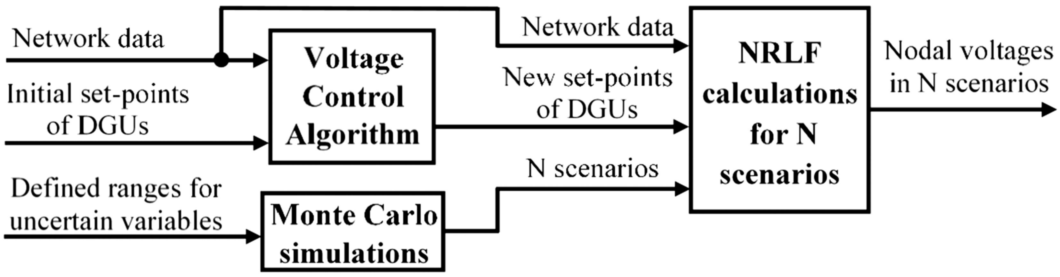

Fig. 1 *Proposed approach to evaluate the model uncertainty impact on the VCA*

independent, exact PF of loads is supposed to be known, system lines are modelled with the series impedances which are supposed to remain unchanged with respect to the loading conditions, and the substation transformer is considered as a pure reactance. Therefore, the corrected voltages obtained by the VCA are subject to the variations due to the utilisation of these simplified models. The main objective of this work is to evaluate the impacts of the uncertain models of the network components on the performance of the studied VCA. In this regard, a three-stage method as shown in Fig. 1 is proposed. It consists of the VCA, MC simulations, and load flow calculations.

The first part of the proposed method is the VCA. It receives the network data and initial values of DGUs powers. If the voltage violations are found in the system, it defines the new set-points of DGUs in order to remove those voltage violations. The new powers of DGUs are kept constant for the further analyses. The second part is the scenarios' creation by the MC simulations. Given that the exact models of the studied components are not available, MC simulations are used to generate N scenarios within the predefined ranges for the parameters of the models under study in order to cover the possible values that those parameters can take in reality. The final stage is the load flow calculations considering the set-points of DGUs obtained by the VCA, N scenarios for the uncertain models of the network components and rest of the network data. The load flow calculations are repeated for each of the N scenarios created by the MC technique. Therefore, finally, N sets of node voltages will be available that will be transformed into the cumulative distribution function (CDF) form. The CDFs of nodal voltages give possible ranges of the voltage variations at the system buses in the generated scenarios. They show also the probability of having a specific voltage value within these obtained ranges. If the CDFs of the system voltages are found to be within the permitted voltage range, it can be concluded that the uncertain models of the studied components will not create voltage violation problem in the VCA. The three parts of the proposed method are described in the following sections.

2.1 Voltage control algorithm

The VCA used in this work has been first introduced in [9, 12]. It is designed to return simultaneously all the violated voltages inside the permitted voltage range by managing the active and reactive powers of DGUs. The voltage regulation problem is linearised by the use of the sensitivity analysis. It is formulated as an optimisation problem, which aims at minimising the total weighted amount of the active and reactive power changes of DGUs subject to the voltage constraints as well as the physical limits of DGUs as

$$\textbf{Min}: \text{OF} = \sum_{x=1}^{N_G} \left(C_Q |\Delta Q_{\text{DGU}x}| + C_P \Delta P_{\text{DGU}x} \right) \quad (1)$$

$$\sum_{x=1}^{N_G} \left(\frac{\partial V_I}{\partial Q_{\text{DGU}x}} \Delta Q_{\text{DGU}x} + \frac{\partial V_I}{\partial P_{\text{DGU}x}} \Delta P_{\text{DGU}x} \right) \geq \Delta \boldsymbol{V}_{\text{proper\_I}} \quad (2)$$

$$\Delta Q_{\text{DGU}x}^{\min} \leq \Delta Q_{\text{DGU}x} \leq \Delta Q_{\text{DGU}x}^{\max} \quad (3)$$

$$0 \leq \Delta P_{\text{DGU}x} \leq |P_{\text{DGU}x}| \quad (4)$$

where N_{G} is a total number of the DGUs that contribute to the voltage regulation problem. $\Delta P_{\text{DGU}x}$ and $\Delta Q_{\text{DGU}x}$ are the active and reactive power changes of the DGU number x. Also, C_P and C_Q are the weighting coefficients for DGUs active and reactive powers, respectively. $\Delta \boldsymbol{V}_{\text{proper\_I}}$ gives the needed values of voltage changes in order to return the violated voltages (V_I) inside the permitted voltage range. Subscript I denotes to all buses with the voltage violations. Therefore, $\Delta \boldsymbol{V}_{\text{proper\_I}}$ is a vector with a number of elements equal to the number of the buses with the voltage violations. The inequality constraint (2) represents the fact that the active and reactive power changes of DGUs must return the violated voltages into the permitted voltage limits. Also, inequality constraints in (3) and (4) indicate the bounds on the active and reactive power changes of DGUs.

The VCA starts with running an initial load flow calculation. If the voltage violations are found in the system, all buses with the voltage violations are selected and $\Delta \boldsymbol{V}_{\text{proper\_I}}$ is composed. Thanks to the application of the voltage sensitivity analysis method, the effects of the DGUs power changes on the system voltages are known. Thus, there is no need to run load flow calculation inside the optimisation problem. The sensitivity coefficients in (2) are defined parameters, the proper values of voltage changes for removing the voltage violations are also defined parameters, but $\Delta Q_{\text{DGU}x}$ and $\Delta P_{\text{DGU}x}$ ($x = 1, 2, \ldots, N_{\text{G}}$) are control variables that must be optimally selected. The linear programming toolbox of MATLAB is used to solve the optimisation problem of the VCA. Once the presented optimisation problem is solved, the needed contributions of DGUs to manage the voltage constraints are defined. Then, a new load flow calculation is done including the new values of DGUs powers. At this stage, the corrected system voltages obtained by the load flow study are plotted and the VCA stops.

2.2 MC simulations

In the literature, the MC technique has been used in order to analyse the uncertain and unobservable nature of the distribution systems. In [13, 14], the MC simulations have been used to study the uncertainty impacts associated with the nodal generations and consumptions. Application of the sensitivity analysis in a probabilistic context based on the MC simulations for characterising the low-voltage distribution systems has been studied in [15]. Also, a state estimation technique has been developed in [16]. The MC simulations are employed to validate the proposed method.

The MC tool used in the current paper is based on the work presented in [13]. In this method, first, the possible variation range of the random (uncertain) variable is defined (for instance $\pm x$). Then, proper number of points are created between the lower and upper bounds of the defined range according to the desired accuracy. It is assumed that the probability of having a point within this range is normally distributed. Therefore, it can be assigned to a normal distribution function [13, 14]. Afterwards, the probability density function corresponding to those points is obtained by calculating their standard deviation and mean value. Also, by definition, a probability density function can be transformed into a CDF using

$$\text{CDF}(x) = P(X \leq x) \quad (5)$$

where X is the random variable associated with the uncertain parameter of the model under study and x is the upper bound on the variation range of the uncertain parameter. To create N scenarios for the parameter of the model under study, a sampling procedure is applied to the obtained CDF as follows [13]. A uniformly distributed random value between 0 and 1 is chosen. It is assigned to the CDF on the vertical axis and its corresponding value on the horizontal axis gives the variation that the uncertain parameter of the model under study can have in one scenario. The sampling procedure is repeated N times in order to create N scenarios. In the end, a vector with N elements is built that covers the possible variations that the uncertain parameter of the model under study can have. Considering the created scenarios and the basic (simplified) model, the uncertain nature of the studied component is taken into account.

2.3 NRLF study

The NRLF study is used in this work in order to evaluate the system voltages in the scenarios created by the MC simulations. In the NRLF, the non-linear algebraic equations of the nodal powers are linearised by expanding them through the Taylor series. It constitutes the so-called Jacobian matrix which gives the linearised relationships between the small changes in the real and reactive powers with respect to the small changes in the nodal voltage angles and magnitudes as below:

$$\begin{bmatrix}\Delta \boldsymbol{P}\\ \Delta \boldsymbol{Q}\end{bmatrix}=\begin{bmatrix}\dfrac{\partial \boldsymbol{P}}{\partial \boldsymbol{\theta}} & \dfrac{\partial \boldsymbol{P}}{\partial \boldsymbol{V}}\\ \dfrac{\partial \boldsymbol{Q}}{\partial \boldsymbol{\theta}} & \dfrac{\partial \boldsymbol{Q}}{\partial \boldsymbol{V}}\end{bmatrix}\begin{bmatrix}\Delta \boldsymbol{\theta}\\ \Delta \boldsymbol{V}\end{bmatrix}=\begin{bmatrix}\boldsymbol{J}_1 & \boldsymbol{J}_2\\ \boldsymbol{J}_3 & \boldsymbol{J}_4\end{bmatrix}\begin{bmatrix}\Delta \boldsymbol{\theta}\\ \Delta \boldsymbol{V}\end{bmatrix} \tag{6}$$

where $\Delta\boldsymbol{\theta}$ and $\Delta\boldsymbol{V}$ denote to the vectors of small variations in the voltage angles and magnitudes at the P–Q buses, respectively. Also, $\Delta\boldsymbol{P}$ and $\Delta\boldsymbol{Q}$ are the vectors of errors between the scheduled and calculated powers at the P–Q buses. The mathematical relations to obtain the elements of the Jacobian matrix have been given in [17]. Once the Jacobian matrix is composed, using $\Delta\boldsymbol{P}$ and $\Delta\boldsymbol{Q}$ which are known parameters and inverted Jacobian matrix according to (6), system voltages are updated. Then, the new voltages are employed to update $\Delta\boldsymbol{P}$ and $\Delta\boldsymbol{Q}$ vectors as well. In the next iteration of the NRLF, the Jacobian matrix elements will be updated in order to obtain the new voltages and eventually new $\Delta\boldsymbol{P}$ and $\Delta\boldsymbol{Q}$. The NRLF in this iterative-based procedure tries to minimise the errors ($\Delta\boldsymbol{P}$ and $\Delta\boldsymbol{Q}$). The iterative procedure stops when a predefined error is met.

3 Studied cases

As stated before, the model based on which the VCA analysis is performed does not represent the real characteristic of the network. There are different factors that have been neglected in the VCA due to the uncertainty, unobservability and complexity of the network model. An accurate and up-to-date network model should incorporate factors such as the working points, loading conditions, ambient temperature, voltage, frequency, ageing of the equipment etc. Given that it is not possible to take all these factors into account, in this paper, the most dominant ones in the medium-voltage (MV) distribution systems are considered. The current investigation focuses on impacts of the uncertainties associated with the voltage dependency of loads, PF of loads, thermal dependency of lines, shunt admittances of lines and internal resistance of the substation transformer on the output results of the considered VCA. The studied cases are described in the following sections.

3.1 Voltage dependency of loads

The load demand in an electric device is rated at the nominal voltage, but regarding the nature of the load, it can vary when the system voltage is not equal to the nominal value. To represent the dependency degree of the load to the voltage, polynomial and exponential models have been widely used in the literature [18–22]. In the polynomial (known also as ZIP) model, a typical load is considered to be a combination of the power constant, current constant and impedance constant loads. The power constant load type is supposed to be independent of the voltage, while the current constant model is a linear function of the voltage, and the impedance constant type is proportional to the square voltage. The polynomial load model is expressed by the following equations for active and reactive powers:

$$P^{*}=P\left[a_P\cdot V^2+b_P\cdot V+c_P\right] \tag{7}$$

$$Q^{*}=Q\left[a_Q\cdot V^2+b_Q\cdot V+c_Q\right] \tag{8}$$

where P and Q stand for the rated active and reactive powers of load at the nominal voltage equal to 1 pu. Also, P^* and Q^* denote the actual consumed active and reactive power values at the voltage equal to V. The coefficients a_P, b_P, c_P, a_Q, b_Q and c_Q of polynomial model determine the voltage dependency characteristic of the load. In the exponential model, the actual consumed active and reactive powers of load (P^* and Q^*) are obtained by

$$P^{*}=P\cdot V^{\alpha} \tag{9}$$

$$Q^{*}=Q\cdot V^{\beta} \tag{10}$$

In the exponential model, voltage dependency of load for active and reactive powers is defined by the exponents α and β, respectively. In this work, in order to study the uncertainty of the load-voltage dependency, the exponential load model is used because of the following reasons. First, in the exponential model, the uncertain variables for active and reactive powers of load are exponents α and β, whereas in the polynomial model there will be three uncertain variables (i.e. a_P, b_P and c_P) for active power and three other variables (i.e. a_Q, b_Q and c_Q) for reactive power of load. Therefore, in the polynomial model, there will be three times more uncertain variables for each of the load buses compared with the case of the exponential model. Second, in the polynomial model, sum of the coefficients in (7) and (8) must be always equal to one ($a_P+b_P+c_P=a_Q+b_Q+c_Q=1$). It means that the scenarios for the polynomial coefficients of active and reactive powers cannot be created independently and one of these three coefficients in (7) and (8) must be always used to make the summation of each three coefficients equal to one. Consequently, it is concluded that the exponential model can be implemented in a more efficient and straightforward manner than the polynomial approach. It is worth noting that the polynomial and exponential models generally lead to quite similar results such that they can be used interchangeably for representing the voltage dependency of load in the MV and low-voltage levels, according to Korunovic *et al.* [21] and Collin *et al.* [22], respectively.

Given that the exact dependency degree of load powers to voltage is unknown, in this paper, MC simulations are employed to create scenarios that can cover the uncertain nature of the loads in a probabilistic way. Two approaches as described in the following sections will be introduced in order to take the voltage dependency of the loads into consideration.

3.1.1 Approach based on the maximum values: In the first approach, the MC simulations are used to create the scenarios that cover the possible variations that the load powers can have due to the voltage dependency. According to (9) and (10), the maximum variations of load powers with respect to the voltage are determined by having the maximum values of α and β as well as the maximum voltage magnitude. In the literature, it is found that based on the load's nature, the voltage dependency exponents can be as big as 2.6 and 4 for α and β, respectively [19, 20]. Taking into account the worst case scenarios for the voltage rise and drop situations, the biggest voltage variations in the studied network (presented in Section 4) would be approximately in the range of ±0.06 pu (around 1 pu). Considering the biggest possible α and β equal to 2.6 and 4 [19, 20], the maximum variations of load active and reactive powers with respect to the voltage in the voltage rise case are equal to +16 and +26% of their nominal values, respectively, according to (9) and (10). Similarly, in the voltage drop state, the extreme variations of load active and reactive powers in function of voltage are given by −15 and −22% of their nominal values, respectively, according to (9) and (10). In the voltage rise case, the lower bounds of load power variations are set to 0 to represent no load-voltage dependency, whereas in the voltage drop case the upper bounds of load power variations are equal to 0 that correspond to zero load-voltage dependency condition. The MC simulations will be used here to create scenarios within the predefined ranges for the load active and reactive power variations with respect to the voltage. It is expected that by having the rated load powers (P and Q) and their variations created by the MC, the uncertain nature of the load-voltage dependency can be properly taken into account.

3.1.2 Approach based on the adapted NRLF study: In the second approach for the investigation on the load model uncertainty, the MC simulations are used to create scenarios for the levels of the voltage dependency of the loads, namely α and β. Therefore, based on the defined ranges for α and β, N scenarios are created for these coefficients. Then, the NRLF study is adapted in order to be able to recognise the load-voltage dependency such that the created α and β in each scenario will be treated to determine the system state in that scenario. Similarly, by evaluating all scenarios, N sets of system voltages are obtained that will be transformed into the CDF form. The NRLF study is modified as follows in order to incorporate the load-voltage dependency.

Assuming that the system loads are voltage dependent, the mathematical relations for calculating the elements of sub-Jacobian matrices ($\boldsymbol{J}_1$, $\boldsymbol{J}_2$, $\boldsymbol{J}_3$ and $\boldsymbol{J}_4$) in (6) should be modified accordingly. In fact, the voltage dependency of loads affects all elements of the sub-Jacobian matrices. Considering (9) and (10), the diagonal elements of $\boldsymbol{J}_2$ and $\boldsymbol{J}_4$ will be obtained by

$$\frac{\partial P_i^*}{\partial V_i} = P_i \cdot \alpha(i) \cdot V_i^{\alpha(i)-1} + \frac{\partial P_i}{\partial V_i} \cdot V_i^{\alpha(i)} \tag{11}$$

$$\frac{\partial Q_i^*}{\partial V_i} = Q_i \cdot \beta(i) \cdot V_i^{\beta(i)-1} + \frac{\partial Q_i}{\partial V_i} \cdot V_i^{\beta(i)} \tag{12}$$

Also, off-diagonal elements of $\boldsymbol{J}_2$ and $\boldsymbol{J}_4$ are given by

$$\frac{\partial P_i^*}{\partial V_j} = \frac{\partial P_i}{\partial V_j} \cdot V_i^{\alpha(i)} \tag{13}$$

$$\frac{\partial Q_i^*}{\partial V_j} = \frac{\partial Q_i}{\partial V_j} \cdot V_i^{\beta(i)} \tag{14}$$

Similarly, the diagonal and off-diagonal elements of $\boldsymbol{J}_1$ are written as

$$\frac{\partial P_i^*}{\partial \theta_i} = \frac{\partial P_i}{\partial \theta_i} \cdot V_i^{\alpha(i)} \tag{15}$$

$$\frac{\partial P_i^*}{\partial \theta_j} = \frac{\partial P_i}{\partial \theta_j} \cdot V_i^{\alpha(i)} \tag{16}$$

Moreover, finally, the diagonal and off-diagonal elements of $\boldsymbol{J}_3$ are obtained by

$$\frac{\partial Q_i^*}{\partial \theta_i} = \frac{\partial Q_i}{\partial \theta_i} \cdot V_i^{\beta(i)} \tag{17}$$

$$\frac{\partial Q_i^*}{\partial \theta_j} = \frac{\partial Q_i}{\partial \theta_j} \cdot V_i^{\beta(i)} \tag{18}$$

Apart from modified formulations of the elements of the sub-Jacobian matrices, the NRLF principles as explained in Section 2.3 remain unchanged for the load flow study incorporating the voltage dependency factor.

In the study based on the adapted NRLF approach, the MC simulations are used to create scenarios for α within the range of 0–2.6 and β in the range of 0–4. Therefore, it is observed that the predefined bounds for α and β are identical to the ones selected in the approach based on the maximum values so that the obtained results of these two approaches can be equally compared later on.

3.2 PF of loads

In the electric distribution systems, due to lack of the sufficient measurements, load PFs cannot be obtained accurately. As a result, an uncertainty is added to the load model regarding the PF. Assuming that the active power load is known, the PF uncertainty affects the reactive power consumption of the load. In this work, in order to study the impact of the uncertainty associated with the load PF, it is supposed that the latter one can vary within a specific range. Then, MC simulations are utilised to create N scenarios for the load PF within that predefined range. The reactive power corresponding to the generated PF in each scenario is calculated using (19). This procedure is followed for all the load buses independently. In the end, vectors of nodal reactive powers are built that can be used to evaluate impacts of load PF uncertainties using the NRLF calculations

$$Q = P \cdot \tan(\cos^{-1}(\text{PF})) \tag{19}$$

where PF stands for the load PF. It should be noted that for the analysis of this part, the voltage dependency of the load is neglected and power constant load model is taken into consideration. Moreover, the variation range of the load PF is supposed to be from 0.9 (lagging) to 1. Within this range, considering the initial average PF of loads (see the Appendix) in the studied system which is equal to 0.98 (lagging), the reactive powers of loads can increase by 138% of their respective initial values when PF is equal to 0.9 or decrease to 0 in the case of unity PF (PF = 1).

3.3 Thermal dependency of the line resistances

The electrical resistance of the line increases with the conductor temperature rise. Therefore, the line resistance depends not only on the conductor size and type, but also on the temperature at which the line conductor is operating [23]. The temperature of the line conductor is in function of the current that passes through the line and the conductor ambient temperature. It means that, according to the actual level of the line loading and the conductor ambient temperature, the line electrical resistance should be recalculated. The overhead lines are more subject to the ambient temperature variations than the underground cable lines. In this work, the studied network consists of underground cables. Thus, it is assumed that the cable loading has a dominant effect on the conductor temperature compared with the impact of the ambient temperature. Given that in the studied network, the actual (up-to-date) temperatures of the cable conductors are not available, we rely on the experimental results reported in [24] to obtain the possible variations that the cable conductor temperatures can have due to current intensity changes.

In [24], a test site has been constructed in order to measure the temperature changes of underground MV power cables with constant and cyclic currents. The experiments have been done on a 15 kV underground cable, which has been placed in the duct bank with the soil temperature equal to 24°C. The maximum ampacity of the studied cable is 600 A. According to the introduced daily load cycle in that work, the cable current is changed from 8 to 83% of its nominal current. Within this range of current variations, the conductor temperature changes between 48 and 85°C. Also, in another test that was performed on the same cable in [24], it is reported that with a constant current equal to 50% of the cable rated ampacity, the conductor temperature reaches 62°C.

In the network studied in this paper, total powers of DGUs are almost three times bigger than sum of the load powers (see the

Appendix). Therefore, the temperature variations of cable conductors as a function of the cable loadings in the voltage rise case are expected to be bigger than ones of the voltage drop state. In the voltage rise case, the branch loadings are close to the maximal ampacities of the cables. As a result, the cable conductor temperatures can increase to 85°C based on [24]. Moreover, due to the ambient temperature in more severe conditions (>24°C), the cable conductor temperatures can go up to 90°C which is usually considered as the maximum permitted temperature of the cable conductor insulation [25]. Assuming that the resistances of the lines have been initially adapted for 62°C (based on the temperature that corresponds to a 50% cable loading), maximal temperature variations of the cable conductors in the voltage rise case will be equal to 28°C (= 90–62). It results in increasing the cable resistances up to 11% of their initial values (at 62°C) by use of (20) [26, 27]. In addition, it is considered that in ambient temperatures below 24°C, the cable conductor temperatures can drop by 10°C which would decrease the line resistances to 4% of their initial values (at 62°C) according to equation below:

$$R_{\text{new}} = R_0 \cdot (1 + \alpha_c \Delta T) \tag{20}$$

where R_0 is the initial cable resistance at 62°C (the temperature corresponding to a 50% cable loading) and R_{new} denotes to the up-to-date cable resistance value by taking the conductor temperature variations (ΔT) around 62°C into account. Also, α_c is the temperature coefficient of resistivity equal to 0.00393 for copper conductors.

In the voltage drop case, the cable loadings hardly exceed 50% of their rated ampacities. In this situation, it can be expected that the temperature variations of the cable conductors due to the loading conditions and ambient temperature changes can fall in a range of ±15°C (around 62°C) that create resistance changes equal to ±5.8% of their initial values using (20).

By having the initial resistances of the lines (at 62°C) and their possible variations (ΔR) obtained by the MC simulations, the uncertainty in the line models due to the thermal dependency effect is taken into account. It is worth mentioning that in this paper, the line inductance is considered constant as it depends mostly on the installation configuration of the cables.

3.4 Shunt admittances of the lines

Shunt admittances of the lines are usually neglected in the distribution systems while they can have important impacts on the system voltages in case of the long cable lines. According to Brenna *et al.* [8], values of the charging capacitance of the lines are found to be in the range of 0.2–0.25 µF/km for the cables with sections varying from 95 to 245 mm^2. Considering the bigger value for the line capacity (0.25 µF/km) and having the length of the lines in the studied network, the upper bounds of the predefined ranges for the admittances of all lines can be determined. Since in the VCA, shunt admittances of the lines have been totally neglected, the lower bounds of the admittance variations will be equal to 0. The MC simulations are employed here to create N scenarios according to the predefined bounds. It should be noted that in each scenario and for each line, the obtained admittance value is divided into two ($b/2$) to be assigned to each side of the corresponding line based on the π equivalent model.

3.5 Internal resistance of the substation transformer

The power transformers are modelled with a series impedance while its resistive part is mostly considered to be negligible. Although internal resistance of the transformer is very small compared with its reactance, it can have considerable effects on the system voltages because of two main reasons. First, in the distribution systems with the high ratio of resistance to reactance, the system voltages highly depend on the branch resistances. Second, the substation transformer is located at the starting point of the network in series with all other buses. Therefore, it has an impact on all nodal voltages. The typical reactance to the resistance ratio of the normal power transformers is found to be in the range of 20–40 [28]. Furthermore, it is considered that the resistance of transformer can vary based on its loading conditions. In this regard, an extension of ±10% with respect to the range mentioned in [28] is adopted. Consequently, in this work, it is supposed that the resistance of the transformer (R_T) can take values from the range starting at 2.25% (1/40 × 0.9) and ending at 5.5% (1/20 × 1.1) of the transformer reactance. It should be noted that the reactance of the transformer is known and kept constant in all scenarios.

3.6 Cumulative uncertainty effects of the load, line and transformer models

In the last section of this work, the cumulative uncertainty effects of the load, line and transformer models on the VCA performance are investigated. In the study on the load model regarding the PF uncertainty in Section 3.2, the power constant load model has been taken into account. However, it is known that the PF of the voltage-dependent load is in functions of α and β since by changing the voltage dependency exponents, the active and reactive powers of load, as well as the load PF will be changed. This must be taken into consideration in (19) when creating vectors of nodal reactive powers. Considering the fact that the load is of voltage-dependent type, we have

$$\begin{aligned}\tan(\cos^{-1}(\text{PF}^*)) &= \frac{Q^*}{P^*} = \frac{Q \cdot V^{\beta}}{P \cdot V^{\alpha}} = \frac{Q}{P} \cdot V^{\beta-\alpha} \\ &= \tan(\cos^{-1}(\text{PF})) \cdot V^{\beta-\alpha}\end{aligned} \tag{21}$$

where PF* and PF stand for the PF in case of voltage-dependent exponential load and power constant load models, respectively. Equation (19) for the voltage-dependent load is rewritten as follows:

$$Q^* = P^* \cdot \tan(\cos^{-1}(\text{PF}^*)) = P \cdot \tan(\cos^{-1}(\text{PF})) \cdot V^{\beta} \tag{22}$$

Therefore, in order to study the PF uncertainty when the load is of the voltage-dependent type, vectors of nodal reactive powers should be built according to (22). It is worth noting that the active powers of loads will be obtained using (9) considering the generated scenarios for α. Apart from this modification, a similar procedure as developed before is followed here to evaluate the cumulative uncertainty associated with the load, line and transformer models. To this end, the scenarios for the uncertain variables, namely α, β and PF for all loads, ΔR and $b/2$ for all lines and R_T for the substation transformer are generated independently using the MC simulations according to the defined range for each of the variables. The system voltages are then evaluated using the adapted NRLF study and the boxplots of obtained voltages will be illustrated eventually.

4 Investigated test system

The proposed method in this work is tested on the 77-bus, 11 kV radial distribution system as shown in Fig. 2 [2, 12]. In this network, the system lines are modelled with the series impedances and the system loads are considered to be voltage independent. There are 22 DGUs connected to the system which are identical with the rated power equal to 3.5 MW. The capability curves of DGUs are obtained from the points given in [9]. In the load flow study, bus number 1 is considered as the slack bus and all other buses are P–Q buses. The substation transformer located between nodes 1 and 2 is modelled with a pure reactance equal to 12.5% pu in the transformer base power (80 MVA). DGUs active power is modelled as a negative load. The permitted upper and lower-voltage limits are 1.03 and 0.97 pu, respectively.

5 Simulation results

The proposed method including the VCA, MC tool, and NRLF study is implemented in the MATLAB environment. The investigation is carried out on the test network as shown in Fig. 2 in the voltage drop and rise states. In this regard, two working

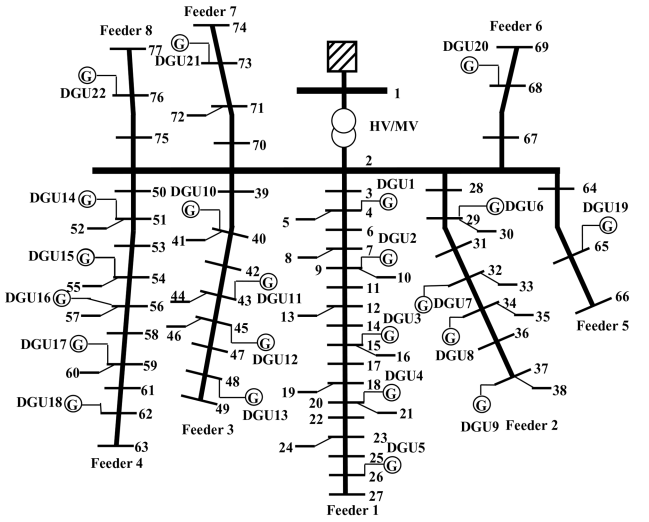

Fig. 2 *77-Bus radial distribution system*

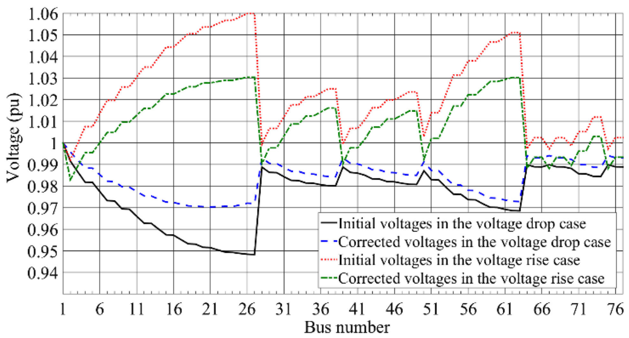

Fig. 3 *Initial system voltages as well as the corrected ones obtained by the VCA in the voltage drop and rise cases*

points as follows are defined in order to create the voltage drop and rise conditions. In the first working point for the voltage drop case, all loads are considered to be at their maximum values while active powers of DGUs are equal to zero. In the second working point corresponding to the voltage rise state, it is supposed that the system loads are at 10% of their respective nominal values and active powers of DGUs are equal to 90% of their rated values. The initial reactive powers of DGUs in both cases are set to zero.

In the proposed method for evaluating the effects of the model uncertainty on the voltage constraints, in the first stage, the violated voltages will be managed using the VCA by relying on the simplified models of the system components as shown in Fig. 1. Thus, the abovementioned working points are given separately to the VCA for the voltage regulation purpose. The initial system voltages, as well as the ones obtained after the voltage regulation by the VCA, are depicted in Fig. 3. Also, Table 1 presents the corrective actions of DGUs in order to manage the voltage violations in both voltage rise and drop cases.

For the voltage regulation in the voltage rise conditions, the reactive power changes of DGUs are preferred to the active power curtailments as mentioned in [2, 7]. In the current work, the weighting coefficient for the reactive power changes of DGUs is set to 1 ($C_Q = 1$), whereas its counterpart for the active power curtailment is considered to be ten times bigger ($C_P = 10$). It should be noted that the generation curtailment of DGUs will not be used for the voltage constraints management in the voltage drop state because it will worsen the voltage violations.

In the studied working point for simulating voltage rise case, voltage violations happen in the feeders 1 and 4 (at buses 11–27 and 54–63) as it can be seen in Fig. 3. To remove these voltage violations, DGU5 and DGU18 which have the highest impacts on the violated voltages are used with their maximum available reactive power (2.31 Mvar). Also, DGU4 and DGU17 provide the rest of the needed reactive powers. In the voltage drop case, the major voltage violations occur at the end of the feeder 1 at buses 9–

Table 1 VCA results in the voltage rise and drop conditions

	Voltage drop	Voltage rise
ΔQ_{DGUx} (Mvar) $x = 1, 2, \ldots, N_G$	DGU5 = −2.717 DGU4 = −0.07	DGU5 = 2.31 DGU4 = 1.09 DGU18 = 2.31 DGU17 = 0.07
ΔP_{DGUx} (MW) $x = 1, 2, \ldots, N_G$	—	—
OF	2.787 (Mvar)	5.781 (Mvar)

27, thus, the VCA employs DGU5 and DGU4 to return those voltages inside the permitted voltage range. The new set-points of DGUs obtained by the VCA are used for further analyses.

The second step of the proposed method is characterising the uncertain model of the studied components. To take into account the model uncertainty associated with each of the individual studied components, a number of 1000 scenarios ($N = 1000$) are generated by the MC simulations for the uncertain variable of the corresponding case according to its predefined range. The system voltages are finally evaluated by the NRLF calculations considering each of the generated scenarios and the new set-points of DGUs reported in Table 1. The voltage results will be presented in the CDF form. In the voltage drop state, the CDF of the voltage at bus 21 is selected for the illustration, because after the voltage regulation the voltage at bus 21 is the closest one to the permitted lower limit (see Fig. 3). As a result, voltage at that bus is more likely to be fallen outside of the permitted voltage range (in response to the model uncertainty) compared with other buses. In the voltage rise case, CDFs of the voltages at buses 26 and 62 are plotted since after the voltage regulation, voltage at these buses are closest ones to the permitted upper-voltage limit. The corrected voltage values obtained by the VCA are 1.0303 and 1.0302 pu for buses 26 and 62 in the voltage rise case, and 0.9703 pu at bus 21 in the voltage drop case. In what follows, first, the model uncertainty effects related to each of the studied components are investigated individually. Then, the cumulative uncertainty effects regarding all the studied factors will be evaluated and the boxplots of the resultant node voltages will be presented.

5.1 On the impact of the voltage dependency of the loads

The uncertainty effect due to the voltage dependency of loads is investigated here by the approaches based on the maximum values and the adapted NRLF study. Figs. 4*a* and *b* show the CDFs of the voltages at the selected buses corresponding to the study on the voltage drop and rise cases.

Considering the results shown in Figs. 4*a* and *b*, it is noted that the uncertainty in the load models due to the voltage dependency effect does not create voltage violation problem in the VCA in both voltage drop and rise cases. It is explained by the fact that the load changes due to the voltage dependency are in the proper direction of the voltage control purpose. According to (9) and (10), in the voltage drop situation, the actually consumed loads are smaller than the rated ones; consequently, the system voltages increase compared with the ones obtained by the rated load values. In the voltage rise situation, the actually consumed loads are bigger than the rated ones; therefore, the node voltages will reduce compared with the ones obtained by the rated load values. It is worth mentioning that the small voltage violations (from 1.03 pu limit) found in the voltage rise case at buses 26 and 62 are not happened because of the voltage dependency of loads. As mentioned before, the corrected voltages obtained by the VCA are 1.0303 and 1.0302 pu at buses 26 and 62. Therefore, in the voltage rise case, the voltage dependency of loads has slightly decreased the voltages at buses 26 and 62 (see Fig. 4*b*).

Furthermore, by comparing Figs. 4*a* and *b*, it is noted that in the voltage drop situation, the load-voltage dependency creates a wider range of the voltage variations compared with the ones in the voltage rise case. This is justified by the fact that in the voltage drop condition, the load powers are maximal, while in the voltage

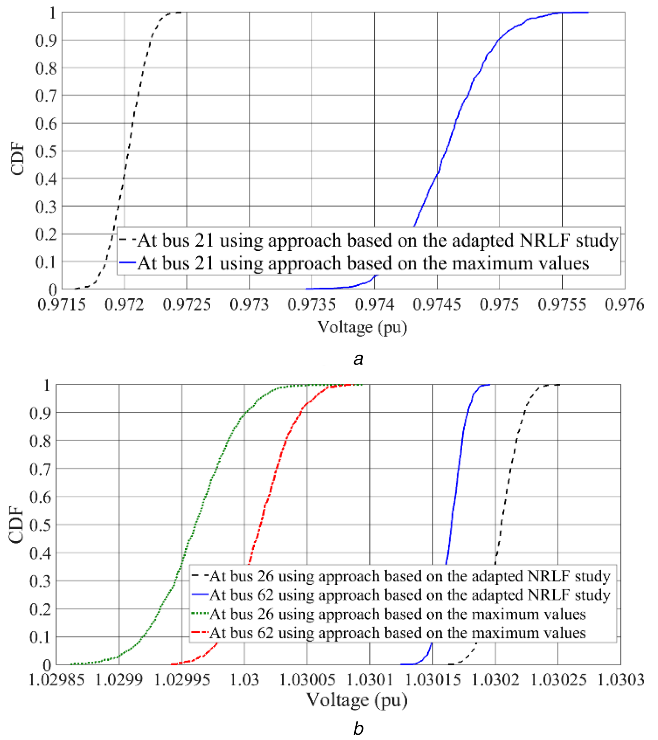

Fig. 4 *CDFs of the voltages at the selected buses obtained by the NRLF study considering the model uncertainty due to the voltage dependency of loads*
(a) In the voltage drop case, ***(b)*** In the voltage rise case

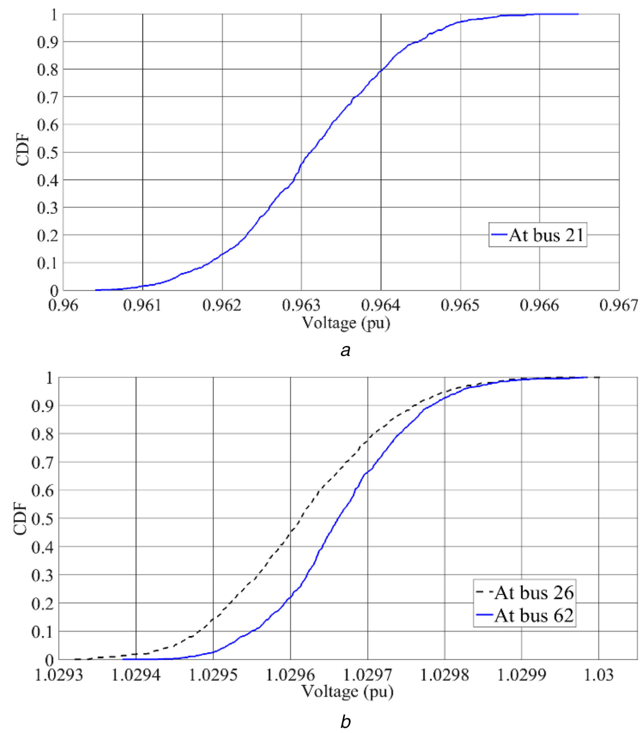

Fig. 5 *CDFs of the voltages at the selected buses obtained by the NRLF study considering the model uncertainty due to the PF of loads*
(a) In the voltage drop case, ***(b)*** In the voltage rise case

rise case loads are at 10% of their nominal values. Consequently, in the former case, loads can have bigger impacts on the system voltages.

Moreover, taking into account the voltage results obtained by the approach based on the maximum values and the ones based on the adapted NRLF study confirms that the latter method leads to more moderate results. For instance, in Fig. 4*a*, due to the voltage dependency of loads, using the approach based on the maximum values, the voltage at bus 21 is found to vary in range of 0.9735–0.9757 pu while for the same case by using the adapted NRLF approach, the voltage variations at that bus are limited to the range of 0.9715–0.9724 pu. Similar results are found also in the voltage rise case in Fig. 4*b*. It indicates that the approach based on the adapted NRLF study determines the impacts of the voltage dependency of loads in a more realistic way than the method based on the maximum values. It is due to the fact that the approach based on the maximum values uses the worst voltage violations to define the range of load variations with respect to the voltage while in another approach, the adapted NRLF study takes into consideration the specific voltages which correspond to the studied working point.

5.2 On the impact of the PF of loads

The impact analysis of the load PF uncertainty is carried out in this section. Fig. 5 presents CDFs of the voltage results at the selected buses when the PF of loads varies within the predefined bound.

Taking Fig. 5*a* corresponding to the voltage drop case into account, it is observed that big voltage violations occur at the 0.97 pu voltage limit. As a minimum effect of the load PF uncertainty, the voltage at bus 21 decreases to 0.9665 pu that means the voltage violation from the permitted lower limit equals to 0.0035 pu. However, the load PF uncertainty can reduce the voltage at bus 21 to 0.9605 pu that is nearly equal to 0.01 pu voltage drop with respect to the initial voltage at bus 21 obtained by the VCA (= 0.9703 pu). On the contrary, in the voltage rise case as it can be seen in Fig. 5*b*, the voltage variations due to the load PF uncertainty have considerably smaller amplitudes and they do not violate the 1.03 pu voltage limit. As the maximum impact of the load PF uncertainty in the voltage rise state, the voltage at bus 26 reduces to 1.0293 pu. With respect to the initial voltage at bus 26 obtained by the VCA (= 1.0303 pu), a voltage drop of 0.001 pu is found at that bus. It is worth mentioning that the load PF uncertainty has a great impact on the voltage drop situation since in that case the load powers are maximal. On the other hand, in the voltage rise case, the load powers are equal to 10% of their nominal values; as a consequence, the eventual effects of the load PF uncertainties are small.

5.3 On the impact of the thermal dependency of the line resistances

The effect of the temperature dependency of the branch resistances is studied in this section. According to the defined ranges for the resistance variations of the cables given in Section 3.3, the MC simulations generate scenarios and the load flow calculations are performed in order to evaluate the nodal voltages. Fig. 6 shows the obtained CDFs of the voltages at the selected buses in the voltage drop and rise conditions.

As it can be observed from Fig. 6*a*, in the voltage drop case, the voltage variations at bus 21 due to the thermal dependency of the line resistances are limited to a range between 0.9691 and 0.9714 pu. Consequently, small voltage violations from the permitted voltage range (its lower bound) are found in the voltage drop case. The voltage amplitude at bus 21 in all the generated scenarios does not go below 0.9691 pu. On the contrary, in the voltage rise case, big voltage violations from the upper permitted voltage limit occur at buses 26 and 62. According to the CDFs of the voltages at buses 26 and 62 as shown in Fig. 6*b*, the voltage at those buses can increase to 1.035 pu due to the impacts of the temperature dependency of the branch resistances. Also, in the generated scenarios, with a probability of 70%, the voltage magnitudes at buses 26 and 62 will be lower than 1.033 and 1.0327 pu, respectively. In Fig. 6, it is clearly seen that the voltage variations in the voltage rise case have a wider range than ones observed in the voltage drop case. It is due to the fact that the predefined ranges for the resistance variations of cables in the voltage rise state are bigger than the bounds of the resistance variations in the voltage drop case.

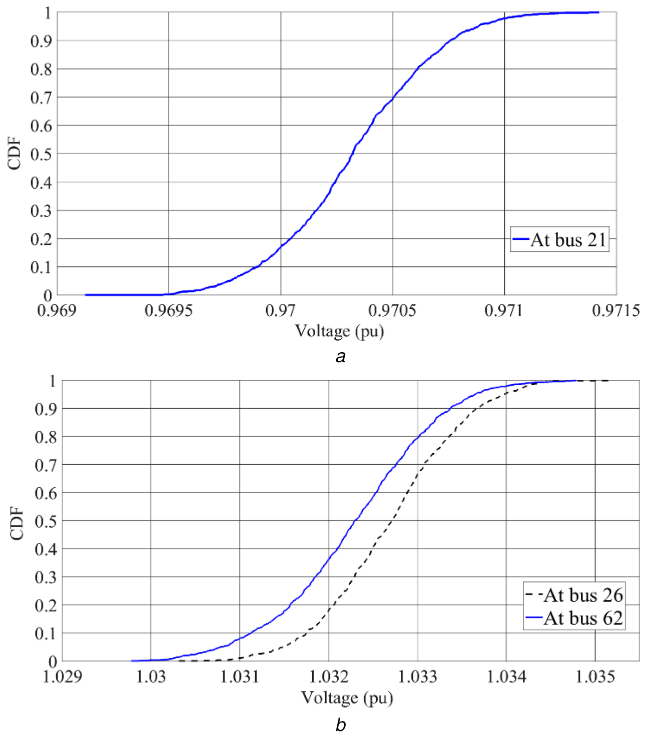

Fig. 6 *CDFs of the voltages at the selected buses obtained by the NRLF study considering the model uncertainty due to the thermal dependency of the line resistances*
(a) In the voltage drop case, ***(b)*** In the voltage rise case

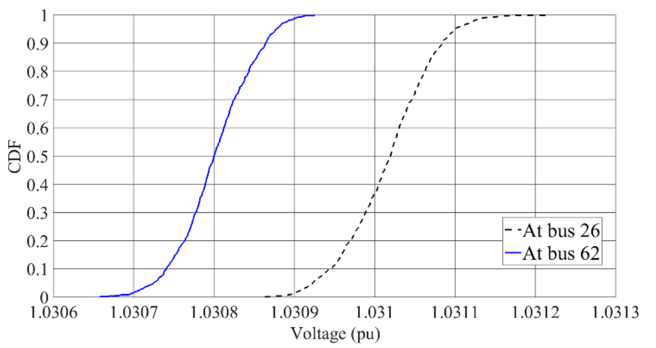

Fig. 7 *CDFs of the voltages at buses 26 and 62 obtained by the NRLF study considering the model uncertainty due to the shunt admittances of the lines in the voltage rise case*

5.4 On the impact of the shunt admittances of the lines

In this section, impacts of incorporating shunt admittances of the lines on the system voltages are studied. It is expected that adding the shunt admittances of the lines will increase the system voltages and can lead to the voltage rise issues. Fig. 7 shows the CDFs of the voltages at buses 26 and 62 obtained by the NRLF study in the voltage rise state considering the scenarios created by the MC simulations.

On the basis of Fig. 7, it is confirmed that adding the shunt admittances of the lines results in the voltage violation from the upper permitted voltage limit in all scenarios created in the voltage rise case. In the simulated scenarios, as the minimum effect of the shunt admittances, the voltage at bus 26 is increased by 0.0006 (= 1.0309–1.0303) pu. The voltage at that bus can reach 1.0312 pu. Concerning impacts of the shunt admittances of the lines on the voltage drop case, it is observed that the system voltages increase similar to the voltage rise case, but with slightly fewer extents. However, since the network is in the voltage drop state, it does not create voltage violation problem.

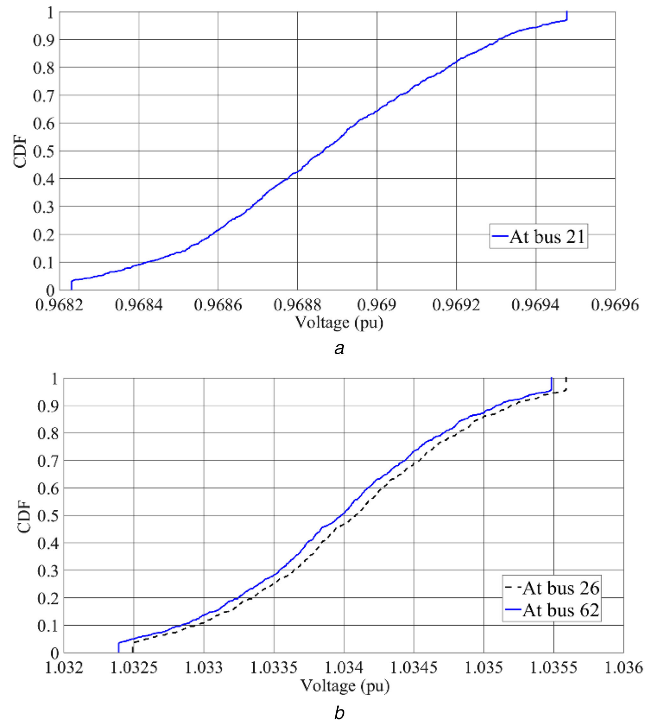

Fig. 8 *CDFs of the voltages at the selected buses obtained by the NRLF study considering the model uncertainty due to the resistance of the substation transformer*
(a) In the voltage drop case, ***(b)*** In the voltage rise case

5.5 On the impact of the internal resistance of the substation transformer

Similar to the previous sections, the investigation on the transformer model uncertainty is carried out on the voltage drop and rise states. Figs. 8*a* and *b* depict the CDFs of the voltages in the corresponding cases when the created scenarios are evaluated by the load flow calculations.

In Figs. 8*a* and *b*, it is seen that the voltage violations occur from both upper- and lower-voltage limits due to the uncertainty that exists in the transformer internal resistance value. In the voltage drop state, the voltage at bus 21 can decrease to 0.9682 pu, and in the voltage rise case voltages at buses 26 and 62 can reach 1.0356 and 1.0355 pu, respectively. Therefore, it is concluded that the internal resistance of the substation transformer has an important influence on the system voltages. In addition, it can be observed from Fig. 8 that the resistance of transformer has a bigger impact on the voltage rise case compared with the voltage drop state. It is due to the fact that in the voltage rise case, the DGUs powers are at their maximum values. As noted before, in the studied test system, the total powers of DGUs are bigger than the total load consumptions.

It is worth mentioning that in Fig. 8*a*, the voltage value corresponding to the starting point of the plotted CDF relates to the scenarios in which the resistance of transformer has been equal to the upper bound of the considered range for R_T. Consequently, it leads to the point with maximum voltage violation. Conversely, the voltages corresponding to the starting point of the plotted CDFs in Fig. 8*b* belong to the scenarios in which the resistance of transformer has been equal to the lower bound of the predefined range for R_T. Therefore, it gives the lower bound of the voltage violations.

5.6 On the cumulative uncertainty impacts associated with the models of the loads, lines and substation transformer

In the last part of this paper, the cumulative uncertainty effects of the load, line and transformer models on the system voltages are investigated. The MC simulations generate scenarios for the studied uncertain variables which are α, β and PF for all loads, ΔR and $b/2$ for all lines and R_T for the substation transformer. Given

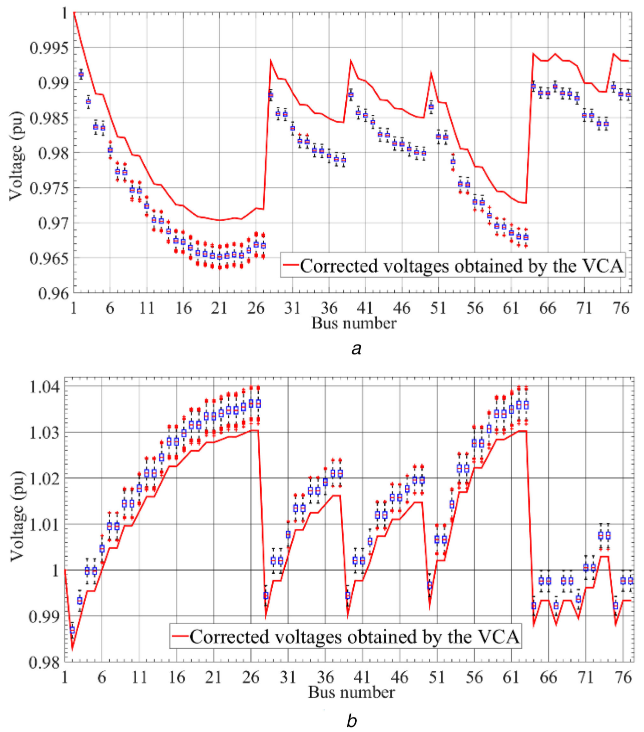

Fig. 9 *Boxplots of the node voltages subject to the cumulative uncertainty effects of the studied components and the corrected voltages obtained by the VCA*
(a) In the voltage drop case, ***(b)*** In the voltage rise case

that there are more uncertain variables, in this case, the total number of scenarios is increased to 5000 in order to be able to capture all the possible realisations of the uncertain variables. The system voltages are obtained using the adapted NRLF study. The boxplots of the node voltages are presented in Fig. 9. The corrected voltages obtained by the VCA (relying on the simplified deterministic models of the system components) are also plotted in the same figure in order to demonstrate clearly how the system voltages can vary as a result of the model uncertainty in the system components.

In Fig. 9*a* corresponding to the investigation on the voltage drop case, it is seen that the boxplots of node voltages exceed the permitted lower-voltage limit. In the study on impacts of each individual uncertain factor, it was found that the voltage dependency of the loads and shunt admittances of the lines lead to the voltage increase while the internal resistances of the substation transformer and load PF decrease the system voltages. Also, the thermal dependency of the lines creates voltage variations around (in both directions) the initial voltages. However, it should be noted that the uncertainty linked to the load PFs has the most dominant effect on the voltage results as shown in Fig. 9*a* and it can be stated that the voltage violations found in the voltage drop case mainly happen due to the PF uncertainty of loads. This latter point can be verified by taking into account the results as shown in Fig. 5*a*, according to which the voltage at bus 21 can decrease to nearly 0.96 pu due to the load PF uncertainty. This big voltage drop has changed in Fig. 9*a* toward more moderate values due to compensating effects of $b/2$, α and β.

In the voltage rise case, the cumulative uncertainty effects of the studied components create big voltage violations above the 1.03 pu voltage limit as it can be seen in Fig. 9*b*. The maximum voltage violation occurs at bus 26, where the voltage amplitude can reach 1.04 pu. With regard to the voltages obtained by the VCA (relying on the simplified models), it is noted that the node voltages can have violations up to nearly 0.01 (= 1.04–1.0303) pu due to the uncertain nature of the models traditionally used for the system components. It is worth mentioning that in the voltage rise case, the uncertainties related to the internal resistance of the substation transformer and the thermal dependency of the branch resistances have the most dominant effects on the node voltages.

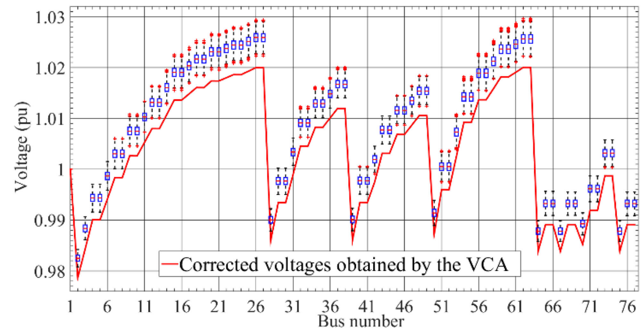

Fig. 10 *Boxplots of the node voltages subject to the cumulative uncertainty effects of the studied components and the corrected voltages obtained by the VCA when the targeted upper-voltage value of the VCA has been modified to 1.02 pu*

The obtained results in this section give us the maximum deviation that the node voltages can have due to the cumulative uncertainty effects of the studied components. This can be utilised in order to reset the targeted voltage values of the VCA in such a way that it makes the VCA robust against possible deviations due to the inherent uncertainty related to the traditionally used (simplified) models of the network components. To do so, in the studied VCA, in order to have the system voltages within the permitted 0.97 pu voltage limit, the targeted lower-voltage value of the VCA should be changed to 0.977 (= 0.97 + 0.007) pu, according to the maximum voltage deviation found in the voltage drop case at bus 21 which is equal to 0.007 pu (see Fig. 9*a*). Similarly, the targeted upper-voltage value of the VCA must be modified to 1.02 (= 1.03–0.01) pu, based on the results shown in Fig. 9*b* regarding the maximum voltage deviation found at bus 26 (= 0.01 pu). In this way, the VCA will be immunised against all possible realisations due to the model uncertainty of the studied components. Fig. 10 shows the boxplots of the system voltages as well as the corrected voltages obtained by the VCA when the targeted upper-voltage value of the VCA is modified to 1.02 pu in order to have the system voltages within the 1.03 pu voltage limit and consequently be robust against the intrinsic uncertainty in the models of the studied components.

As it can be seen in Fig. 10, in all created scenarios that take the model uncertainty effects into account, the system voltages do not violate the 1.03 pu predefined voltage limit when applying the control actions undertaken by the VCA relying on the simplified models of the network components. Similar results can be obtained also when the targeted lower-voltage value of the VCA is changed to 0.977 pu in order to have a robust solution against the possible voltage violations due to the model uncertainty of the system components in the voltage drop case. On the other hand, as a consequence of modifying the targeted voltage bounds of the VCA, a conservative solution will be obtained by the VCA. To make it clearer, in the studied working point for the voltage rise state, when the targeted upper-voltage value of the VCA is set to 1.02 pu, the VCA asks DGU5 and DGU18 to change their reactive powers by 2.31 Mvar. Also, DGU4 and DGU17 provide 2.275 and 1.543 Mvar inductive reactive powers. The objective function of the VCA, in this case, equals to 8.438 Mvar which is bigger than the one presented in Table 1 (5.781 Mvar) when the targeted upper-voltage value was 1.03 pu. The difference between the objective functions in these two cases indicates the control efforts that should be added (or the price that we should pay) in order to make the VCA solutions fully robust against the effects of the studied model's uncertainty in the voltage rise case. Alternatively, in order to avoid a conservative solution, a lower level of the robustness can be adopted that will result in some unwanted voltage violations.

The idea presented in this section suggests an efficient approach to deal with the model uncertainty in the VCA. It should be noted that when the model uncertainty is transferred inside the VCA based on the robust optimisation formulation (e.g. [11]), a long processing time will be added to the VCA execution time in order to characterise the uncertain models of the network components and to evaluate their effects. As a consequence, the VCA may not be any more compatible with the requirement of the real-time voltage management. In this regard, in the current paper, it is suggested to keep the VCA simple (relying on the simplified deterministic network model) which helps us to have (<0.1 s) the VCA results quickly. Thanks to the proposed framework of this paper, the possible deviations that the system voltages can have due to the model uncertainty are known. This information will be utilised eventually to establish a desired level of robustness against the studied model's uncertainty.

6 Conclusion

In this work, a probabilistic framework based on the MC simulations is developed in order to characterise the uncertain models of the network components. The investigation aims at quantifying the impacts of the uncertain models traditionally used for the loads, lines and substation transformer on the voltage constraints of the studied VCA. On the basis of the simulation results, it is concluded that the voltage dependency of loads does not cause voltage violation issues in the VCA. On the contrary, the load PF uncertainty creates big voltage violations in the voltage drop case. Moreover, it is found that adding the shunt admittances of the lines results in increasing the system voltages and it can lead to voltage violation problem in the voltage rise state. Furthermore, it is shown that the internal resistance of the substation transformer and the thermal dependency of the branch resistances have very considerable impacts on the system voltages in such a way that by taking them into account, voltage violations occur from both upper and lower-voltage limits. Finally, through evaluating the cumulative uncertainty effects of the studied components in the tested system, it has been demonstrated that the voltage violations from the permitted voltage range happen in both voltage drop and rise states. To avoid the voltage violations due to the model uncertainty impact, the targeted values of the VCA should be adjusted according to the results of the study on the cumulative uncertainty effects of the studied components.

7 Acknowledgments

The authors thank Professor Thierry Van Cutsem, research director of the fund for scientific research (F.N.R.S) in Belgium, for his constructive ideas and advice during the preparation of this work.

8 References

[1] Capitanescu, F., Bilibin, I., Romero Ramos, E.: 'A comprehensive centralized approach for voltage constraints management in active distribution grid', *IEEE Trans. Power Syst.*, 2013, **29**, (2), pp. 933–942
[2] Valverde, G., Van Cutsem, T.: 'Model predictive control of voltages in active distribution networks', *IEEE Trans. Smart Grid*, 2013, **4**, (4), pp. 2152–2161
[3] Borghetti, A., Bosetti, M., Grillo, S., *et al.*: 'Short-term scheduling and control of active distribution systems with high penetration of renewable resources', *IEEE Syst. J.*, 2010, **4**, (3), pp. 313–322
[4] Christakou, K., LeBoudec, J.Y., Paolone, M., *et al.*: 'Efficient computation of sensitivity coefficients of node voltages and line currents in unbalanced radial electrical distribution networks', *IEEE Trans. Smart Grid*, 2013, **4**, (2), pp. 741–750
[5] Vovos, P.N., Kiprakis, A.E., Wallace, A.R., *et al.*: 'Centralized and distributed voltage control: impact on distributed generation penetration', *IEEE Trans. Power Syst.*, 2007, **22**, (1), pp. 476–483
[6] Zhou, Q., Bialek, J.W.: 'Generation curtailment to manage voltage constraints in distribution networks', *IET Gener. Transm. Distrib.*, 2007, **1**, (3), pp. 492–498
[7] Pilo, F., Pisano, G., Soma, G.G.: 'Optimal coordination of energy resources with a two-stage online active management', *IEEE Trans. Ind. Electron.*, 2011, **58**, (10), pp. 4526–4537
[8] Brenna, M., De Beradinis, E., Delli Carpini, L., *et al.*: 'Automatic distributed voltage control algorithm in smart grids applications', *IEEE Trans. Smart Grid*, 2013, **4**, (2), pp. 877–885
[9] Bakhshideh Zad, B., Hasanvand, H., Lobry, J., *et al.*: 'Optimal reactive power control of DGs for voltage regulation of MV distribution systems using sensitivity analysis method and PSO algorithm', *Int. J. Electr. Power Energy Syst.*, 2015, **68**, pp. 52–60
[10] Bahramipanah, M., Cherkaoui, R., Paolone, M.: 'Decentralized voltage control of clustered active distribution network by means of energy storage systems', *Electr. Power Syst. Res.*, 2016, **136**, pp. 370–382
[11] Christakou, K., Paolone, M., Abur, A.: 'Voltage control in active distribution networks under uncertainty in the system model: a robust optimization approach', *IEEE Trans. Smart Grid*, 2017, **PP**, (99), p. 1–1, DOI: 10.1109/TSG.2017.2693212
[12] Bakhshideh Zad, B., Lobry, J., Vallée, F.: 'A centralized approach for voltage control of MV distribution systems using DGs power control and a direct sensitivity analysis method'. Proc. 2016 IEEE Int. Energy Conf., Belgium, 2016
[13] Vallée, F., Klonari, V., Lisiecki, T., *et al.*: 'Development of a probabilistic tool using Monte Carlo simulation and smart meters measurements for the long term analysis of low voltage distribution grids with photovoltaic generation', *Int. J. Electr. Power Energy Syst.*, 2013, **53**, pp. 468–477
[14] Conti, S., Raiti, S.: 'Probabilistic load flow using Monte Carlo techniques for distribution networks with photovoltaic generators', *Sol. Energy*, 2007, **81**, (12), pp. 1473–1481
[15] Klonari, V., Bakhshideh Zad, B., Lobry, J., *et al.*: 'Application of voltage sensitivity analysis in a probabilistic context for characterizing low voltage network operation'. Proc. 2016 Int. Conf. Probabilistic methods Applied to Power Systems, China, 2016
[16] Singh, R., Pall, P.C., Jabr, R.A.: 'Distribution system state estimation through Gaussian mixture model of the load as pseudo-measurement', *IET Gener. Transm. Distrib.*, 2010, **4**, (1), pp. 50–59
[17] Saadat, H.: '*Power system analysis*' (McGraw-Hill, New York, NY, USA, 1999)
[18] Haque, M.H.: 'Load flow solution of distribution systems with voltage dependent load models', *Electr. Power Syst. Res.*, 1996, **36**, (3), pp. 151–156
[19] Mithulananthan, N., Salama, M.M.A., Cañizares, C.A., *et al.*: 'Distribution system voltage regulation and Var compensation for different static load models', *Int. J. Electr. Eng. Educ.*, 2000, **37**, (4), pp. 384–395
[20] Van Cutsem, T., Vournas, C.: '*Voltage stability of electric power systems*' (Springer, Boston, MA, USA, 2008)
[21] Korunovic, L.M., Stojanovic, D.P., Milanovic, J.V.: 'Identification of static load characteristics based on measurements in medium voltage distribution network', *IET Gener. Transm. Distrib.*, 2008, **2**, (2), pp. 227–234
[22] Collin, A.J., Tsagarakis, G., Kiprakis, A.E., *et al.*: 'Development of low-voltage load models for the residential load sector', *IEEE Trans. Power Syst.* 2014, **29**, (5), pp. 2180–2188
[23] William, A.B.: 'A guide to installation of medium voltage cable', *IEEE Trans. Ind. Appl.*, 1977, **IA-13**, (6), pp. 527–529
[24] Bernath, A., Olfe, D.B., Ferguson, B.W.: 'Heat transfer measurements on unequally loaded underground power cables with constant and cyclic currents', *IEEE Power Trans. Power Appar. Syst.*, 1984, **PAS-103**, (10), pp. 2799–2806
[25] '6–36 kV medium voltage underground power cables' Nexans Medium Voltage Underground Cables, 2010
[26] 'Medium voltage cables', Catalogue available at http://www.nexans.com/Lebanon/2011/mediumvoltage_2.pdf
[27] Bakshi, U.A., Bakshi, M.V.: '*Power system-I*' (Technical Publications, Pune, India, 2009)
[28] ANSI/IEEE C37.010-1979: 'IEEE application guide for AC high-voltage circuit breakers rated on a symmetrical current basis', 1989

9 Appendix

The main characteristics of the 77-bus United Kingdom Generic Distribution System are as follows:

Number of loads: 75.
Total active power of the loads: 24.274 MW.
Total reactive power of the loads: 4.854 Mvar.
Average PF of loads: 0.98.
Total active power productions of DGUs = 77 (22 × 3.5) MW.
Total length of the system lines: 56.82 km.
Longest feeder of the system: feeder 1, 11.15 km.
Average resistance of the lines: 0.0886 Ω/km.
Average reactance of the lines: 0.0502 Ω/km.